



## HYDROPHILIC CARBOHYDRATE NANOCAPSULES AS A SUSTAINED DELIVERY DEPOT OF SMALL AND MACROMOLECULAR DRUGS: PREFORMULATION AND MASS TRANSFER

Arindam Basu Sarkar\*, Gregory M. Kochak

Department of Pharmaceutical Sciences, The University of Findlay, Findlay, OH 45840, United States of America.

\*Corresponding author's E-mail: [basusarkar@findlay.edu](mailto:basusarkar@findlay.edu)

Accepted on: 06-01-2012; Finalized on: 20-02-2012.

### ABSTRACT

Preformulation studies incorporating tartrazine, a small molecule, and lysozyme, a macromolecule, into carbohydrate nanocapsules were performed. The nanocapsules were synthesized using interfacial poly-condensation. Partition behavior, interfacial aggregation of lysozyme, and factors controlling release of incorporated molecules were analyzed. Molecular release from the nanocapsules was analyzed under sink conditions and modeled with a heterogeneous mass transfer model.

**Keywords:** Lysozyme, Release, Modeling, Carbohydrate, Nanoparticles, Interfacial Crosslinking.

### 1. INTRODUCTION

Carbohydrate polymers, both charged and uncharged have been used historically in drug delivery research to achieve controlled delivery. Charged carbohydrate polymers, like anionic alginates,<sup>1</sup> pullulan<sup>2</sup> and cationic chitosan<sup>3</sup> have all been used to produce microspheres as drug delivery platforms. The use of nonionic carbohydrate polymers like starch,<sup>4</sup> high amylose starch<sup>5</sup> and dextran<sup>6-8</sup> for drug delivery has been gaining acceptance in recent years. Microspheres have been prepared with alginic acid by utilizing the ionic interactions between the carboxylic acid groups in the polymer and di or trivalent metal ions like  $\text{Ca}^{+2}$  or  $\text{Al}^{+3}$ . The limitation of these systems is that the ionic interaction is reversible and the integrity of the microspheres are compromised in the presence of other ionic species like citrates, phosphates,  $\text{Na}^+$ ,  $\text{K}^+$  and  $\text{Mg}^+$ , which are normally present in physiological fluids. The resulting disintegration of nanocapsules on exposure to physiological fluids causes rapid release of encapsulated bioactive molecules. Polyion condensation has been used to produce micro/nanocapsules with chitosan and DNA for potential use as non-viral DNA delivery vectors. Apart from the fact that all cationic polymers including chitosan possess considerable toxicity,<sup>3</sup> chitosan microspheres are also made through ionic interactions and thus suffer from similar limitations as alginates. A variety of different crosslinking agents have been used to produce micro/nanocapsules by crosslinking nonionic carbohydrate polymers throughout the device. Crosslinking in the bulk, especially with strong crosslinking agents like glutaraldehyde<sup>9</sup> is always associated with concerns of reacting the encapsulated bioactive compound itself and thus denaturing and/or immobilizing them in the particle.

In an attempt to address these concerns, carbohydrate nanocapsules have been prepared using a novel emulsion/interfacial crosslinking reaction.<sup>10</sup> The main advantage of this platform is that the encapsulated

bioactive molecules potentially remain in a benign microenvironment at the core of the device unaffected by the interfacial crosslinking. Another important aspect of this drug delivery system (DDS) is that being made up of carbohydrate polymers, this DDS has a hydrophilic surface which is expected to minimize if not eliminate the activation of the reticuloendothelial system and thus the removal of the particles from blood stream through phagocytosis when introduced into the body. In a previous study we have shown that in terms of interfacial physical properties the carbohydrate nanocapsules are hydrophilic and therefore compatible with aqueous matrices resulting in no aggregation.<sup>10</sup>

The object of the current research is to investigate complexities involved with the incorporation of bioactive molecules in nanocapsules and their subsequent *in vitro* release from the particles in simulated physiological fluids. Two molecules have been chosen for the encapsulation to represent the two extreme ends of the molecular weight spectrum of bioactive molecules. Tartrazine, a hydrophilic small molecule, containing strong anionic groups, is chosen to represent traditional small drug molecules. Chicken egg white lysozyme is a moderately large protein (molecular weight 14,700) with native stereo structures. Lysozyme has a large hydrodynamic diameter of 4.1 nm.<sup>11</sup> It is a relatively hydrophobic protein carrying a net cationic charge at pH 9 and below and has been chosen to represent the emerging group of polypeptides and proteins that are increasingly emerging as drug molecules. The main goals pursued in this effort are to maximize encapsulation efficiency and quantitatively describe the mechanism of drug release (mass transfer).



## 2. MATERIALS AND METHODS

### 2.1. Materials

The carbohydrate polymers were procured from a variety of commercial sources and used without further purification. The polymers include corn starch (CS) (Sigma, St. Louis, MO), waxy maize starch (WMS) (PFP 2850, Cargill Foods, Minneapolis, MN), maltodextrin (MA) from waxy maize starch (C\*Dry 01955, Cerestar USA Inc., Hammond, IA), and maltodextrin (MCS) from corn starch (Maltrin M40, Grain Processing Corporation, Mucatine, IA). The crosslinkers include terephthaloyl chloride (TC) (Sigma-Aldrich, St. Louis, MO), and trimesoyl chloride (TMC) (Across organics, Pittsburg, PA). Other chemicals include sorbitan-mono-palmitate (Span-40), buffer salts (Sigma-Aldrich, St. Louis, MO), chloroform (CL), cyclohexane (CH), methylene chloride (MC), acetone, and ethanol (Fisher Scientific, Pittsburg, PA). All solvents were of ACS grade. Dimethyl sulfoxide (DMSO), acetonitrile (ACN), tetrahydrofuran (THF), and dimethyl formamide (DMF) were used as high pressure liquid chromatography (HPLC) solvents. Triethylamine (TEA), phenacyl bromide (PB), sodium azide (SA) are other reagents (Fisher Scientific).

Organic phase one (OP-1) was prepared by dissolving 6 % (w/v) Span 40 in a mixture of cyclohexane and chloroform (68/32, v/v) as the continuum phase of the emulsion. Organic phase two (OP-2) was prepared by dissolving requisite amount of TC and TMC in cyclohexane and chloroform (68/32, v/v) for carrying out the crosslinking.

### 2.2. Preparation of nanocapsules and incorporation of tartrazine

Carbohydrate nanocapsules were prepared by an interfacial polyesterification reaction as earlier described.<sup>10</sup> Tartrazine nanocapsules were made using different combinations of CS, WMS and maltodextrins MCS and MA as polymers with TC and TMC and with maltodextrins MCS and MA as polymers and TC as crosslinkers.

**Table 1:** Effect of carbohydrate polymer on the encapsulation efficiency of tartrazine

Crosslinker Concentration (w/v, %)	Polymer Concentration (w/v, %)	Encapsulation Efficiency of Tartrazine (%)
TMC (1.635)	Corn Starch (4)	39.1
TMC (1.635)	Waxy maize starch (5)	32.4
TC (1.25)	Corn starch (4)	39.1
TC (1.25)	Waxy maize starch (5)	39.6
TC (1.25)	MCS (50)	78.4
TC (1.25)	MA (45)	83.9

Briefly, the carbohydrate polymers CS, WMS, MCS and MA were heated in an appropriate volume of buffer in screw capped bottles to produce carbohydrate colloids in the case of high molecular weight carbohydrates, and true solutions in the case of maltodextrins. The concentration of carbohydrate polymers (Table-1) was

maintained close to their maximum solubility. The pH of the aqueous phase was maintained at 10.0 by using 200 mM borate buffer to maximize the encapsulation of tartrazine. The colloid or solution was allowed to cool to room temperature while stirring before tartrazine was incorporated at a concentration of 10% (w/w) relative to the polymer.

Twenty (20.0) mL of the carbohydrate colloid/solution was emulsified in 100 mL of OP-1 in a Silverson LR-4<sup>®</sup> homogenizer at 5,000 rpm for 1 minute. The emulsion was then poured into 100 mL of OP-2. The reaction was continued for 24 hr. The final concentration of both the crosslinkers was ~55 mM in the organic phase. The reaction was stopped by pouring the reaction mixture into 700 mL of ethanol in a 1000 mL beaker while stirring. The precipitated nanocapsules were washed 3 times with ethanol and 3 times with acetone by repeated centrifugation at 1,500 g and vortexing following discontinuation of stirring. Finally, the suspension of nanocapsules in acetone was dried under vacuum at 14.0 psi at room temperature (20-25°C) overnight.

### 2.3 Encapsulation and release studies with tartrazine

Two hundred and twenty (220) mg of dry nanocapsules with a theoretical load of 9.09% of tartrazine was dispersed in 5 mL of 100 mM potassium phosphate buffered saline (KBPS) at pH 7.4. The theoretical loading of tartrazine was determined by the following equation.

$$\text{Theoretical load of tartrazine} = \left[ \frac{\text{Weight of tartrazine} * 100}{\text{Weight of dry nanoparticles}} \right]$$

Nine percent (approximate) load corresponded to 10% (w/w) relative to carbohydrate weight. The suspension was immediately placed into an 18 cm long dialysis membrane tube (SpectraPor<sup>®</sup>, Spectrum Laboratories Inc., Rancho Dominguez, CA; molecular weight cutoff of 50,000 Daltons). One end of the dialysis tube was clamped securely. The suspension was then added to the pouch and the other end was clamped such that the distance between the two clamps was 5 cm in each case. The lower clamps had a magnetic weight built in so that the formed pouch floats upright and remains stable during stirring. The pouch containing the suspended nanocapsules was placed in a 1000 mL beaker containing 495 mL of 100 mM KBPS. To minimize evaporation of the dissolution media, the beakers were covered with a thin polyethylene sheet (Clingwrap<sup>®</sup>). A multiple head magnetic stirrer with precise control was used to maintain a stirring speed of 150 rpm. One (1.0) mL samples were withdrawn at predetermined time intervals and the media replenished each time. Tartrazine was quantified by absorbance spectroscopy using a Beckman UV/VIS spectrophotometer at 445 nm wavelength. To account for any possible contribution of the dialysis membrane to tartrazine delivery, 20 mg of tartrazine was dissolved in 5 mL of 100 mM KPBS (4 mg/mL). The aliquot was placed into dialysis tubing as previously described and used as the control.



At the end of the release studies, the asymptotic level of tartrazine concentration was used for encapsulation efficiency based on:  $E = (A/T) \cdot 100$ , where E is the encapsulation efficiency, A is the actual amount of tartrazine released and T is the amount (9.09 %) of tartrazine added.

## 2.4 Partitioning and interfacial aggregation of lysozyme

In order to ensure maximum loading of lysozyme in the carbohydrate nanocapsules, preformulation studies were performed to establish the effect of organic solvents used as the continuum phase, pH, and carbohydrate load in the dispersed aqueous phase on lysozyme partitioning. Firstly, 4.5 % (w/v) lysozyme was dissolved in deionized water. The pH of the deionized water was adjusted to 3.0, 4.0 and 5.0 by adding 50, 20, 10  $\mu\text{L}$  of 10 % (v/v) trifluoroacetic acid. The final concentration of trifluoroacetic acid was 0.65, 0.26, and 0.13 mM, respectively. Since lysozyme is a basic protein with an isoelectric pH of 11.0,<sup>12</sup> pH values chosen are expected to fully ionize the amino groups resulting in minimum partitioning into the continuum phase. Twenty (20) mL of this aqueous phase was homogenized with 100 mL of methylene chloride, cyclohexane, chloroform or cyclohexane/chloroform (68/32, v/v). Surfactant was deliberately omitted from the preformulation study to ensure adequate separation of the phases. The homogenized phase was allowed to separate on standing overnight at room temperature. After the phases separated, 1.0 mL samples were collected from the aqueous phase, centrifuged at 1,500 g to remove any insoluble aggregated lysozyme and analyzed by HPLC.

## 2.5 Incorporation of lysozyme in nanocapsules

Lysozyme was incorporated in nanocapsules made from maltodextrin obtained from waxy maize starch (MA). The crosslinker used was TMC. The preparation procedure used was similar to the process already described. Only the modifications will be mentioned in this section. Forty five (45) percent (w/v) of MA was dissolved in the aqueous phase buffered at pH 3.0 by heating. Unless stated otherwise, 4.5 g of lysozyme was added to 100 mL of MA solution after cooling to room temperature. The solution was slowly stirred until the lysozyme dissolved. A final theoretical loading of 9.09 % (w/w) was obtained corresponding to 10% lysozyme relative to carbohydrate load. Nine (9) g of lysozyme was added to the same volume of MA solution in some batches to achieve a theoretical lysozyme loading of 16.67 % (w/w) corresponding to 20% lysozyme relative to carbohydrate. The TMC concentration was varied from 0.8 to 565 mM in the continuum phase.

## 2.6 Lysozyme assays

### 2.6.1 Assay of lysozyme from release samples

Standard protein solutions were made in the concentrations of 1, 5, 10, 20, 30 and 40  $\mu\text{g}/\text{mL}$  in 100 mM (KPBS) containing 0.2 % (w/v) sodium azide (SA). To account for any interference from the nanocapsules in

authentic samples, blank nanocapsules were suspended in the standard solution in the same concentration used in the release experiments. As a low molecular weight carbohydrate scavenger, 75  $\mu\text{L}$  of n-butanol was added to 1.0 mL of the sample in a 1.5 mL polypropylene micro centrifuge tube. The samples were then centrifuged at 14,000 g for 15 min to separate any precipitated carbohydrate residue and the suspended nanocapsules. Approximately 250  $\mu\text{L}$  of the supernatant was then transferred to autosampler vials. Seventy (70)  $\mu\text{L}$  of the sample was injected for HPLC analysis. Both the lysozyme standards and samples from release studies were identical to one another in composition except for the lysozyme content.

The stationary phase was a Zorbax SB300<sup>®</sup> column with 5  $\mu\text{m}$  particle size, 300  $\text{\AA}$  pore size,  $C_{18}$  packing, and with 4.6 x 150 mm column dimension. A 4.6 x 10 mm precolumn of the same stationary phase composition was used as a protective device. The mobile phase was composed of 57 % (v/v) of solvent A and 43 % (v/v) solvent B pumped at a flow rate of 1.0 mL/min. Solvent A was composed of deionized water containing 0.1 % (v/v) trifluoroacetic acid (TFA). Solvent B was composed of 4 % (v/v) DMSO, 20 % (v/v) THF, 76 % (v/v) ACN, and 0.1 % (v/v) TFA.

The chromatography was carried out at ambient temperature. The chromatographic system consisted of a Thermo Separation (San Jose CA, USA) Model P2000 pump used in the isocratic mode, a Model AS3000 autoinjector, and a Model FL2000 variable-wavelength fluorimetric detector. The detection was carried out at 280 nm excitation and 340 nm emission wavelengths. Lysozyme eluted at 4.2 min.

Calibration curves were evaluated in a concentration range of 1 - 40  $\mu\text{g}/\text{mL}$ . The accuracy (mean) of the method was within  $\pm 5\%$  at all concentration levels within this range, while the precision (RSD) was within 5% at all calibration levels except at 1  $\mu\text{g}/\text{mL}$  (20%). Calibration curves were constructed between 5 and 40  $\mu\text{g}/\text{mL}$  for analysis of all release study samples.

### 2.6.2 Content assay of lysozyme

For quantifying nanoparticle lysozyme content, a slight modification of the HPLC sample preparation method was adopted for optimum efficiency. An appropriate amount of dry nanocapsules were dispersed in 1.0 mL of 100 mM KPBS containing 0.2 % (v/v) SA. The suspension was diluted with 2.0 mL of deionized water and 1.0 mL of mobile phase, mixed for 2 min in a vortex mixer, and kept for 1 hr at room temperature. A 70  $\mu\text{L}$  aliquot was injected. The DMSO present in the mobile phase was found to dissolve the nanocapsules. A calibration curve was constructed and used for this purpose in the range of 1-30  $\mu\text{g}/\text{mL}$ . The sample amount of the nanocapsules was adjusted to maintain lysozyme concentrations within the calibration range.

Calibration curves were evaluated in a concentration range of 1 - 40  $\mu\text{g}/\text{mL}$ . The accuracy (mean) of the method



was within  $\pm 10\%$  at all concentration levels within this range, while the precision (RSD) was within 5% at all calibration levels except at 1  $\mu\text{g/ml}$  (24%). Some peak tailing was observed when lysozyme was encapsulated when compared to lysozyme neat standards. Calibration curves were therefore constructed between 5 and 30  $\mu\text{g/ml}$  and based on peak height.

## 2.7 Crosslinker assay

The degree of substitution of TC and TMC were measured by an appropriate reverse phase HPLC method<sup>13</sup> developed specifically for this purpose.

## 2.8 Release studies with lysozyme

Lysozyme release was evaluated from a dispersion of nanocapsules at pH 7.4 in 100 mM KPBS. The dialysis membrane was omitted since prolonged mass transfer was observed for non-encapsulated lysozyme solution even when using a 100,000 Da molecular weight cutoff dialysis membrane. Two hundred and twenty (220) mg of dry nanocapsules containing lysozyme were dispersed in 500 mL of 100 mM KPBS containing 0.02 % (w/v) of SA in a 1000 mL conical flask. To avoid evaporation of the aqueous media, the flask was covered with a thin polyethylene sheet (Clingwrap®). Sink conditions were maintained by a volume of 500 mL of release media and stirring the media at 150 rpm. Release studies were carried out at room temperature (25°C). One (1.0) mL of sample was withdrawn at predetermined time points for quantification. The samples were handled as described in the lysozyme assay and 70  $\mu\text{L}$  of the sample was injected for analysis by HPLC. Each of the release experiment was repeated thrice and the data points represent the arithmetic mean of the three.

## 2.9 Regression analysis and model assessment for lysozyme release

Nonlinear least-squares regression was used to analyze the underlying mechanism of lysozyme release based on a spherical diffusion model. Initially a unimodal homogeneous diffusion model<sup>14</sup> was used. However, best fit statistical analysis demonstrated the discrimination of two independent modes of lysozyme diffusional release. As a consequence, a heterogenous diffusional model was adopted for subsequent analysis as described by the following equation:

$$\frac{M_t}{M_\infty} = \frac{M_{1,\infty}}{M_\infty} \left( 1 - \frac{6}{\pi^2} \sum_{n=1}^{\infty} \frac{1}{n^2} e^{-P_1 n^2 t} \right) + \frac{M_{2,\infty}}{M_\infty} \left( 1 - \frac{6}{\pi^2} \sum_{n=1}^{\infty} \frac{1}{n^2} e^{-P_2 n^2 t} \right)$$

$$P_1 = \frac{D_1 \pi^2}{r^2}, \quad P_2 = \frac{D_2 \pi^2}{r^2} \quad (1)$$

Here, ' $M_t$ ' is the mass of lysozyme released at time ' $t$ ', ' $M_\infty$ ' is the mass of lysozyme released at infinite time, ' $n$ ' is the summation index varying from one to infinity, ' $P$ ' is the permeability coefficient, ' $D$ ' is the diffusion coefficient of lysozyme, ' $r$ ' is the mean radii of the spheres and the term  $M_t/M_\infty$  denotes fractional release of lysozyme at

time ' $t$ '.  $M_{1,\infty}$  is the mass of lysozyme released by mode 1 at infinite time,  $M_{2,\infty}$  denotes the mass of lysozyme released by mode 2 and  $M_\infty$  is the total mass of lysozyme released.

A ten-term truncation of the infinite series was used. The series coefficient ( $6/\pi^2$ ) was appropriately adjusted to a value of 0.64536 corresponding to the reciprocal sum of the first ten terms of the series at  $t = 0$ .

All curves were analyzed using normalized and nominal data where  $M_\infty$  was estimated from the numerical average of the last 2-3 asymptotic data values. Residual sum of squares was weighted using a factor of 1.0 for regression analysis. The parametric values of  $P_1$ ,  $P_2$ ,  $f_1$ , and  $f_2$  were estimated, where  $f_1 = M_{1,\infty}/M_\infty$  and  $f_2 = M_{2,\infty}/M_\infty$ , and  $f_1 + f_2 = 1$ .

## 3. RESULTS

### 3.1 Encapsulation and release of tartrazine: The effect of polymers

The encapsulation efficiency of tartrazine varied depending on the polymer /oligomer molecular weight (Table 1). All the starches are macromolecules with molecular weights up to million Daltons while the average molecular weight of the maltodextrins (MA and MCS) are 3200 Daltons. Nanocapsule batches prepared from high molecular weight carbohydrate polymers CS and WMS showed relatively low encapsulation efficiency of 32 to 39 % of the incorporated tartrazine irrespective of the crosslinker used. Nanocapsules made from carbohydrate oligomers MCS and MA showed higher encapsulation efficiencies of 78 and 84 %, respectively. As the molecular weight of the carbohydrate polymer increases, the solubility decreases. While oligomers like maltodextrins are freely soluble in dispersed phase (45 - 50 %, w/v), polymers like CS or WMS have a limited solubility (4 - 5%, w/v). This difference in polymer concentration in the dispersed phase has a profound impact on the encapsulation efficiency of small molecules due to entrapment effect as discussed below.

Following completion of the crosslinking reaction, the dispersed aqueous phase was extracted in a large volume of ethanol resulting in a rapid precipitation of the polymer. Though tartrazine is not soluble in any of the solvents, cyclohexane, chloroform or ethanol, it is extractable from the nanocapsules in the presence of small amounts of water provided by the dispersed phase. The small amount of tartrazine remained in the nanocapsules prepared from CS and WMS because it was entrapped in the rapidly precipitating polymers. The entrapment effect of the encapsulated tartrazine was low for CS and WMS because of the low polymer loads. In the cases of MCS and MA, the entrapment effect of the carbohydrate is much more pronounced due to a ten-fold higher carbohydrate concentration [45-50 % (w/v)] in the aqueous phase, made possible by their greater aqueous solubility.



Although some differences in tartrazine release were observed relative to the specific carbohydrate used for encapsulation, comparative tartrazine delivery relative to the control was unremarkable. These results indicate that the encapsulating membrane offers little resistance to tartrazine diffusional mass transfer. A comparison (Figure 1) of the tartrazine release from nanocapsules synthesized with TC and TMC shows that the branched polymer amylopectin (WMS contains >99% amylopectin while corn starch contains only ~61% amylopectin) imparts more resistance to the diffusional release of model small molecule tartrazine irrespective of the crosslinker species.

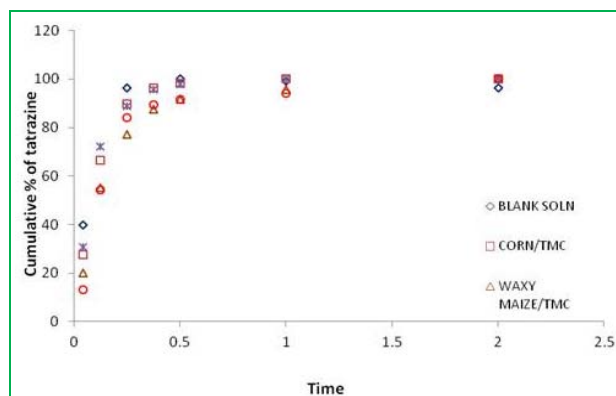


**Figure 1:** Comparative release profiles of tartrazine from nanoparticle batches with different carbohydrate polymers and crosslinkers.

### 3.2. Partitioning of lysozyme and its encapsulation efficiency

The results of lysozyme partitioning experiments using methylene chloride, cyclohexane, chloroform and cyclohexane/chloroform [68/32, (v/v)] at pH values 3.0, 4.0, and 5.0, showed that lysozyme partitioning had a pronounced dependence on both pH and the choice of continuum phase solvent. When MC was used as the continuum phase (Table 2), no lysozyme was detected in the aqueous phase following emulsification and phase separation at any pH tested. Insoluble aggregated lysozyme was observed at the interface and also in both phases. Lysozyme partitioning into the organic phase and aggregation at the interface were found to be low when CH and CL were used separately as the organic phase. The soluble lysozyme, recovered from the aqueous phase following emulsification and phase separation, were 73 and 75 % for CH and CL, respectively, at pH 3.0. However recovery of soluble lysozyme in the aqueous phase was 10 % when CH/CL [68/32, (v/v) %] was used as the continuum phase at pH 3.0. Also, the percentage of soluble lysozyme decreased rapidly with the increase in pH in all cases in which lysozyme was detected in the aqueous phase. The observation of progressively lower recovery of lysozyme from dispersed phase as the pH increased could be attributed to the lower degree of protonation of the amino groups of lysozyme. The optimum pH for encapsulation is 3.0.

**Table 2:** Effect of pH and organic phase solvent on the partitioning behavior of lysozyme. Water-organic phase ratio is 1:5.

Solvent	Lysozyme remaining in aqueous phase (%)		
	pH 3.0	pH 4.0	pH 5.0
Methylene chloride	*ND	ND	ND
Cyclohexane	73.26	44.08	37.4
Chloroform	74.9	21.26	14.03
Cyclohexane: Chloroform [68:32, (v/v)]	9.95	7.16	4.69

Thus, for incorporation of lysozyme, CL was selected as the continuum organic phase and the pH of the dispersed aqueous phase was selected to be 3.0. Lysozyme is known to be stable for several weeks at low acidic pH.<sup>15</sup>

In order to investigate the effect of carbohydrate content on lysozyme partitioning, studies were conducted with 15, 30 and 45 % (w/v) of MA in the aqueous dispersed phase at pH 3.0 with CL as the organic continuum phase. The results show a near quantitative recovery of soluble lysozyme in the aqueous phase following emulsification and phase separation with all levels of carbohydrate in contrast to 75 % recovery from the identical phase system without any carbohydrate (Table 3). These results lead to the conclusion that high carbohydrate load causes lysozyme retention in the dispersed phase due to a carbohydrate-protein interaction. Table 4 shows the actual lysozyme encapsulation efficiency measured in representative batches. The encapsulation efficiency averaged  $98 \pm 10.2$  % of the added lysozyme in a wide range of degree of substitution values.

**Table 3:** Effect of carbohydrate content on the chloroform/water partitioning behavior of lysozyme at pH 3.0 and phase ratio of 5:1.

Aqueous phase Description	Lysozyme remaining in aqueous phase (%)
0% (w/v) polymer (MA)	74.9
15% (w/v) polymer (MA)	95.3
30% (w/v) polymer (MA)	97.3
45% (w/v) polymer (MA)	100

### 3.3. Effect of lysozyme load and reaction specifications on the degree of substitution

The  $f_m$  was found to be proportional to the crosslinker concentration up to about 16 mM irrespective of lysozyme load (Figure 2). Based on theoretical considerations, the interfacial reaction will remain focused at the emulsion interface provided that excess water is available throughout the core to quench the polyesterification reaction along the radius. This condition corresponds with linear reaction kinetics (i.e., pseudo first-order). Correspondingly, this condition was met in the present system up to about 16 mM TMC concentration in the continuum phase with a 24-hr reaction time. At concentrations greater than 16 mM TMC, deviation from linearity suggests depletion of water in the internal phase and/or excess accumulation of trimesic acid in the core. Trimesic acid is the hydrolysis

product of the reaction between TMC and water. Depletion of water in the core marks the transition from interfacially focused synthesis to ordinary bulk synthesis where polyesterification throughout the core is expected. However,  $f_m$  was found to be dependent on the crosslinker concentration as well as the lysozyme load when the crosslinker concentration is increased beyond 16 mM. This observation suggests the presence of some lysozyme at the interface. At a significantly large protein load, presence of lysozyme at the interface probably interferes with crosslinking. This effect may practically limit protein loading in nanocapsules.

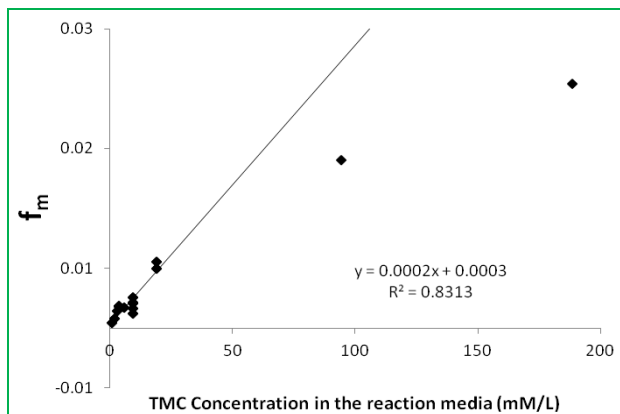


**Figure 2:** Relationship between degree of substitution ( $f_m$ ) and trimesoyl chloride (TMC) concentration (mM) in the continuum phase. The regression line represents the linear range of reaction kinetics for nanocapsule fabrication.

### 3.4 Lysozyme modeling and the extent of release

Residual analysis using a homogeneous diffusion model resulted in systematic trends which lead to the conclusion that a homogeneous diffusion model was found inadequate to explain lysozyme release (Figure 3). Using this model either the first part or the terminal part of the release curve could be fitted with accuracy. Lysozyme release from hydrophilic thin films have been found to be ‘anomalous’ by simple unimodal Fick’s diffusion model. Other investigators<sup>16</sup> have used a two step model development approach to address the divergence from unimodal Fickian diffusion model.

Lysozyme mass transfer was adequately described by a heterogeneous diffusion model incorporating two independent modes of release. Resulting fitted curves (Figure 4) all show high correlation with coefficients ( $R^2$ ) >

0.985 and random residuals, thereby validating the model.

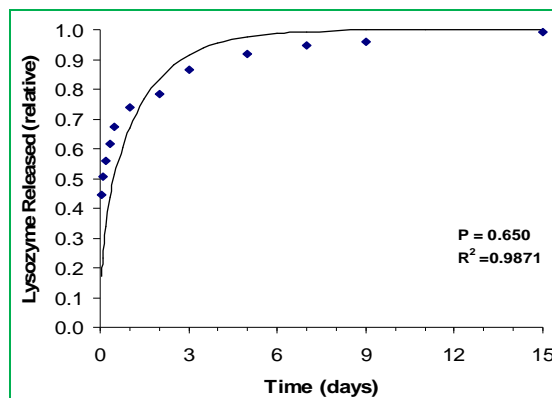


**Figure 3:** Fitting of the lysozyme release profile data from a representative batch with unimodal homogeneous diffusion model. P denotes the predicted permeability coefficient.

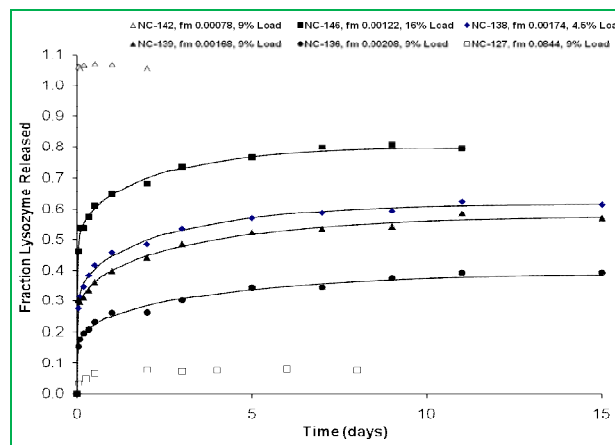


**Figure 4:** Comparative release profiles of lysozyme from nanocapsule batches with different degrees of substitution and protein load. NC-xxx refers to the batch numbers.

Lysozyme release profiles correspond to the combined effect of two individual diffusional pathways characterized by  $P_1$  and  $P_2$ . The mass transfer rate from the first pathway, characterized by  $P_1$ , is very fast and is complete within approximately three hours in all cases (Table 4). The mass transfer rate from the second pathway, characterized by  $P_2$ , is slower. The diffusional release due to the second mode was sustained and continuous for 7-11 days.

**Table 4:** Regression and disposition parameters of lysozyme encapsulation and mass transfer

Batch #	Encapsulation Efficiency (%)	$*f_m$ (%)	Regression parameters					$R^2$	$**f_{total}$
			$P_1$	$P_2$	$f_1$	$f_2$			
NC-127	91.2	8.4						0.08	
NC-136	95.4	0.21	41.8	0.198	0.41	0.59	0.986	0.39	
NC-139	109	0.17	593	0.239	0.47	0.53	0.991	0.53	
NC-138	111	0.17	35.3	0.294	0.48	0.52	0.994	0.61	
NC-146	98.5	0.12	48.8	0.371	0.60	0.40	0.991	0.79	
NC-142	96.3	0.08						1.07	

$*f_m$ , degree of substitution;  $**f_{total}$ , fraction of the asymptotic total released lysozyme relative to the load.



The permeability coefficient  $P_2$ , corresponding to the slower mode of lysozyme release, was found to be related to  $f_m$  (Figure 5). This finding suggests that the slower mode of lysozyme release may be due to the resistance provided by a molecular polymerized network encapsulating lysozyme.

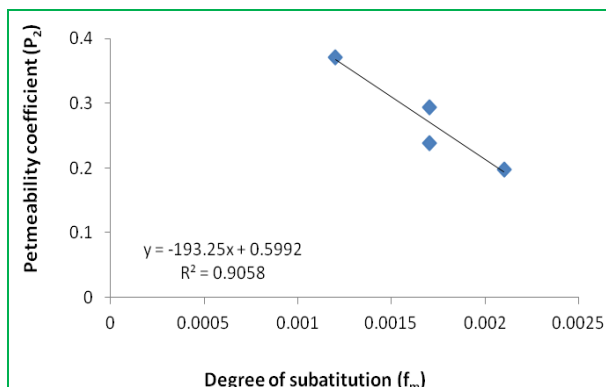


**Figure 5:** Relationship between the permeability coefficient,  $P_2$ , and the degree of substitution.

In addition, the fraction of deliverable lysozyme released by this pathway,  $f_2$ , was correlated with  $f_m$  and increased with a corresponding increase in the degree of substitution (Figure 6). As the degree of substitution  $f_m$  increases, the hydrophilic nanoparticle matrix is more heavily crosslinked. During this crosslinking process, some lysozyme will definitely be crosslinked as well. As the degree of crosslinking increases, the fraction of crosslinked lysozyme should increase. Lysozyme crosslinking is more likely happen through labile amide bonds which undergo slow hydrolysis. This effect can reasonably explain the positive correlation between the  $f_m$  and the  $f_2$  as well as the negative correlation between  $f_m$  and  $P_2$ . It is to be noted that in a complicated process like interfacial crosslinking of carbohydrate colloid containing soluble lysozyme, the parallel reactions like carbohydrate crosslinking and lysozyme crosslinking will take place. Additionally, entanglement of lysozyme in the crosslinked carbohydrate (without any covalent bond) is a possibility.

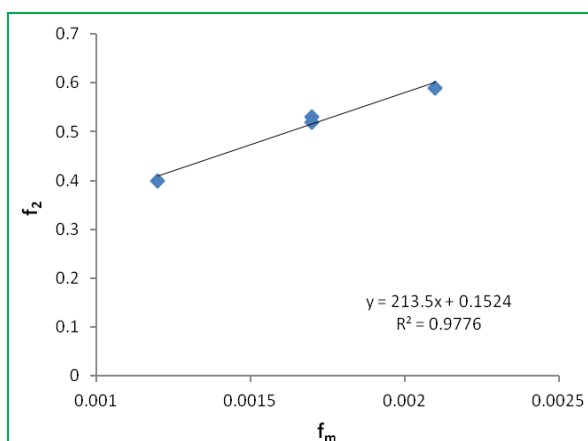


**Figure 6:** Relationship between deliverable lysozyme by the  $f_2$  pathway and the degree of substitution.

The  $f_2$  and  $P_2$  are more likely the total impact of all these effects. The incomplete release of lysozyme from crosslinked nanoparticles discussed in the following section, points to the possibility of mixed mode reaction.

$P_1$  was found to be independent of  $f_m$ , and  $f_1$  decreased as the degree of substitution increased. The rapid mass transfer from this pathway corresponding with  $P_1$  and lack of correlation with the degree of substitution indicates that lysozyme entrapment in these channels have relatively open access to the environment with little mass transfer resistance. There was essentially no difference between the lysozyme mass transfer rate associated with this pathway and mass transfer from nanoparticles produced with minimal polymerization (Batch NC-127). Since 40-60% of lysozyme was released from this pathway within 3 h, rapid mass transfer may be related to the initial swelling of the hydrogel nanocapsule and expansion of these channels, displacing lysozyme through open pores (superficial membrane defects) in the polymer network. This is supported by the observation of other researchers<sup>16</sup> modeling lysozyme release kinetics from hydrophilic thin films. It has been shown that carbohydrate nanocapsules increase in volume 4-5 fold when hydrated compared to the condensed phase.<sup>17-19</sup>

The total extent of lysozyme release was profoundly dependent on  $f_m$  (Figure 7). As the degree of substitution increased, there was a corresponding shift in deliverable lysozyme from the  $f_1$  to the  $f_2$  pathway. Although a shift to the  $f_2$  pathway may be considered desirable since it is associated with prolonged lysozyme release and predictable permeability which can be controlled by modifying  $f_m$  through the reaction conditions, it is at the expense of total lysozyme release. By mass balance, where  $f_{total}$  is the asymptotic total released lysozyme relative to the load,  $1-f_{total}$  is immobilized lysozyme due to co-polymerization which increases with the degree of substitution. If polymer-controlled passive diffusion is the intended mechanism of controlling protein delivery, only a narrow range of degree of substitution values correspond with observed properties of continuously prolonged delivery without excessive immobilization. In the case of lysozyme, a suitable compromise is found in Batch NC-146 with  $f_m$  equal to 0.12% and total deliverable lysozyme at about 80%.

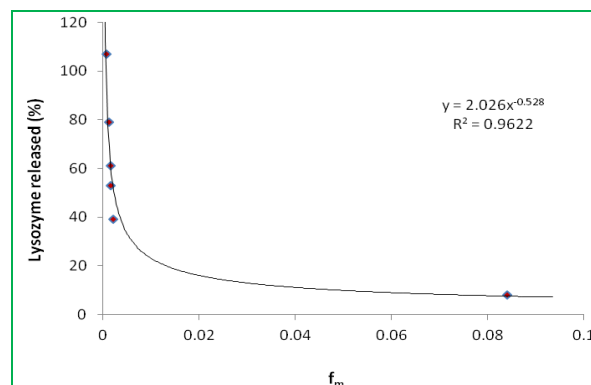


**Figure 7:** The relationship between the extent of lysozyme release ( $f_{total}$ ) and the degree of substitution.

The degree of lysozyme loading affects the total degree of polymerization,  $f_m$ , and the inclusion fraction associated with the  $f_2$  pathway. Comparatively, a 17% lysozyme load reduces  $f_m$  and  $f_2$  relative to 4.5% and 9% loads. The increase in  $P_2$  observed for the 17% load is mechanistically because  $f_m$  is reduced. These results indicate that lysozyme-carbohydrate condensation is less reactive than carbohydrate polymerization alone.

#### 4. DISCUSSION

Hydrophilic polymers are gaining acceptance as the preferred non-viral vectors for drug delivery and cellular intervention because they possess physical chemical interfacial properties compatible with physiological fluid. They do not aggregate,<sup>10</sup> and are spared from opsonization by the reticuloendothelial system.<sup>20,21</sup> Covalently bonded polymers can be regulated synthetically, and therefore potentially impart material properties and control over drug delivery and cellular intervention. They are also stable in physiological environments when compared to ionically coacervated polymers or other self-assembly systems which are completely dependent on the local environment and dissociate in accord with prevailing factors such as pH and competitive associative or complexation ligands. The main problem with hydrophilic polymers is that they apparently offer little resistance to the mass transfer of entrapped drug molecules<sup>17</sup> because of swelling<sup>18,19</sup> and in the case of acrylic acid polymers, are toxic *in vivo*.<sup>22,23</sup> In contrast, carbohydrate polymers and their degradation products are safe *in vivo*.

In the series of studies reported herein, we investigated the notion that mass transfer in nanoparticulate systems composed of hydrophilic polymer networks may be regulated by the degree of substitution of condensation crosslinkers creating a tertiary structured meshwork which would impart controllable resistance (both physical and chemical) to drug release, and in particular, to the release of macromolecules. Using a spatially focused interfacial polyesterification reaction with concomitant internal quenching, we also investigated the degree to which a protein can be spared immobilization due to co-polymerization with carbohydrate.

The condensation reaction of carbohydrates with tri functional TMC at the emulsion interface is a complicated reaction. Many different products are possible. Mono, di or tri esterification as well as inter chain crosslinking, intra chain crosslinking, and chain elongation of the carbohydrate polymers are all possible. A crosslinking reaction involving at least two acid chloride groups is the goal of the interfacial esterification reaction. But it is dependent upon the availability of alcoholic hydroxyl groups of the carbohydrate polymers at the interface and in the right spatial arrangement with respect to the crosslinker molecule. The hydroxyl groups of the carbohydrate polymers have to be present at the interface in sufficient concentrations so that the groups are available for reaction. When lysozyme, as well as with

all other proteins, is additionally incorporated in the internal phase, an amide formation as a result of the reaction between acid chloride groups of the crosslinker and free amino groups of the protein is also possible. This side reaction may also be aided by the fact that lysozyme, like most moderate sized proteins, has some surfactant activity and tends to migrate to the interface.

Preformulation studies showed that interfacial migration of lysozyme can be eliminated by providing sufficient charge to maximize ionization and aqueous solubility, and by providing a sufficient oligomer carbohydrate concentration. Ionization alone does not inhibit interfacial accumulation of protein. The carbohydrate-protein interaction inhibits mass transfer to the emulsion interface. The concentration of oligomer carbohydrate required to insure a homogenous internal phase concentration of protein provides a baseline value for carbohydrate polymerization. These findings demonstrate the importance of preformulation studies in assessing the capability to produce a core-shell polymer system.

Mechanistic mass transfer evaluation was able to discriminate two independent pathways of lysozyme release. Both pathways and lysozyme immobilization were highly dependent on the degree of substitution of TMC. For larger protein molecules like lysozyme with a hydrodynamic diameter 4.1 nm, molecular impedance to mass transfer is consistent with a polymer meshwork model since  $P_2$  and  $f_2$  were strongly correlated with the degree of substitution. As was demonstrated, a balance between protein immobilization and shift to the  $f_2$  pathway where maximal resistance to diffusional mass transfer is achieved would be required to develop a viable hydrophilic polymer-based macromolecular delivery system. Of course, optimal material and mass transfer properties will depend on the specific protein of interest and require experimental assessment. Nevertheless, our findings demonstrate the viability of developing a suitable carbohydrate based macromolecular delivery system provided that *in vivo* cellular intervention can be ascertained. Alternatively, by maximizing  $f_m$ , a completely immobilized protein system can be developed which would require activation though enzymatic degradation of the polymer. Since esterase and amylase enzymes are available *in vivo*, and cellular uptake of conjugated chitosan nanoparticles has been demonstrated<sup>24</sup> this would be a completely viable delivery system.

Assessing the mass transfer properties determined in this study, a supra-structural model consistent with our results would include entrapped lysozyme residing in inclusion zones which are molecularly encapsulating and offering maximal resistance to mass transfer, and entrapped lysozyme residing between inclusion zones that have access to defects in the superficial membrane structure or are infiltrating pores which offer little resistance to mass transfer, particularly when swollen. Whether this compartmentalized polymer network is superficial or extends deeply into the core cannot be





determined from the present study, but warrants further investigation.

Tartrazine is a hydrophilic small molecule. The effect of polymeric carbohydrate encapsulation on tartrazine release was unremarkable. Little resistance to mass transfer was observed when compared to a control solution, although delivery was sustained for about 12 h. However, in this study, a dialysis membrane was utilized, and the mass transfer rate of tartrazine was not directly determined. The observed mass transfer rate of tartrazine can be attributed to the resistance of the dialysis membrane.

## 5. CONCLUSION

In conclusion, we have evaluated factors that affect the synthesis, material properties, and mass transfer characteristics of polymeric carbohydrate-based nanocapsules and provide a framework for further development, particularly regarding macromolecule delivery. This platform is also suitable as a scaffold to enhance further development of interventional modalities *in vivo*. Ultimately, the potential of this platform will depend on the biological and pharmacokinetic disposition of carbohydrate nanocapsules in the systemic circulation, their ability to protect bioactive macromolecules from enzymatic degradation, and their interventional ability at the cellular level.

**6. Acknowledgement:** This work has been done in the Department of Pharmacal Sciences, Harrison School of Pharmacy, Auburn University, Auburn, AL.

## 7. REFERENCES

- Gombotz, WR and Wee, SF. Protein release from alginate matrices. *Advanced Drug Delivery Reviews* 3: 1998; 267-285.
- Mocanu G, Mihai D, Picton L, LeCerrf D and Muller G. Associative pullulan gels and their interaction with biological active substances. *Journal of Controlled Release* 83: 2002; 41-51.
- Richardson SCW, Kolbe HVJ and Duncan R. Potential of low molecular weight mass chitosan as a DNA delivery system: biocompatibility, body distribution and ability to complex and protect DNA. *International Journal of Pharmaceutics* 178: 1999; 231-243.
- Morah LP. Microspheres as nasal drug delivery systems. *Advanced Drug Delivery Reviews* 29: 1998; 185-194.
- Lanaerts V, Moussa I, Dumoulin Y, Mebsout F, Chouard F, Szabo, P, Mateescu, M A, Cartilier L and Marchessault R. Cross-linked high amylose starch for controlled release of drugs: recent advances. *Journal of Controlled Release* 53: 1998; 225-234.
- Mehvar R. Dextran for targeted and sustained delivery of therapeutic and imaging agents. *Journal of Controlled Release* 69:2000; 1-25.
- Stenekes RJH, Loebis AE, Fernandes CM, Crommelin DJA and Hennink WE. Degradable dextran microspheres for controlled release of liposomes. *International Journal of Pharmaceutics* 214: 2001; 17-20.
- Franssen O, Stenekes RJH and Hennink WE. Controlled release of model protein from enzymatically degrading dextran microspheres. *Journal of Controlled Release* 59: 1999; 219-228.
- Tabata Y and Ikada Y. Synthesis of gelatin microspheres containing interferon. *Pharm. Res.* 6: 1989; 422-427.
- Basu Sarkar A, Umesh K and Kochak GM. Interfacially Assembled Carbohydrate Nanocapsules: A Hydrophilic Macromolecule Delivery Platform. *Journal of Biomedical Nanotechnology* 5(5): 2009; 456-463.
- Jensen M, Hansen PB, Murdan S, Frokjar S and Florence AT. Loading into and electro-simulated release of peptides and proteins from chondroitin 4-sulphate hydrogels. *European Journal of Pharmaceutical Sciences* 15:2000; 139-148.
- Alderton G, Ward W and Febold H. Isolation of lysozyme from chicken egg white. *Journal of Biological Chemistry* 157: 1945; 43.
- Basu Sarkar A and Kochak GM. HPLC analysis of aliphatic and aromatic dicarboxylic acid cross-linkers hydrolyzed from carbohydrate polyesters for estimation of molar degree of substitution. *Carbohydrate Polymers* 59: 2005; 305-312.
- Kim C. Controlled release dosage form design. Lancaster, Pennsylvania: Technomic Publishing Company Inc, USA: 20-22.
- Van-Seuningen I, Hayem A and Davril M. Analysis of the conformation and stability of human bronchial lysozyme by circular dichroism. *International Journal of Biochemistry* 24 (4): 1993; 593-598.
- Bunoucore GG, Del Nobile MA, Panizza A, Bove S, Battaglia G, Nicholais L. Modeling the Lysozyme Release Kinetics from Antimicrobial Films Intended for Food Packaging Applications. *Journal of Food Science* 68 (4): 2003; 1365-70.
- Gutowska JS, Bark JS, Kwon IC, ChaY and Kim SW. Squeezing hydrogels for controlled oral drug delivery. *Journal of Controlled Release* 48: 1997; 141-148.
- Korsmeyer RW, Gurny R, Doelker E, Buri P and Peppas NA. Mechanism of solute release from porous hydrophilic polymers. *International Journal of Pharmaceutics* 15: 1982; 25-35.
- Harland RS, Gazzaniga A, Sangalli ME, Colombo P and Peppas NA. Drug/Polymer Matrix Swelling and Dissolution. *Pharmaceutical Research* 5 (8): 1988; 488-494.
- Gaur U, Sahu SK, De TK, Maitra A, Ghosh PK. Biodistribution of fluoresceinated nanoparticles evading reticuloendothelial system. *International Journal of Pharmaceutics* 1-2: 2000; 1-10.
- Torchilin VP. Polymer-coated long circulating microparticulate pharmaceuticals. *Journal of Microencapsulation* 15 (1): 1998; 1-19.
- Silver EH and Murphy SD. Potentiation of Acrylate Ester Toxicity by Prior Treatment with Carboxylesterase inhibitor Triorthotolyl Phosphate (TTP). *Toxicol. And Appl. Pharmacol.* 57 (2): 1981; 208-219.
- Miller RR, Young JT, Kociba RJ, Keyes DJ, Bonder KM and Calhaun LL. Chronic Toxicity and Oncogenicity Bioassay of Inhaled Ethyl Acrylate in Fisher 344 Rats and B6c3f1 Mice. *Drug and Chemical Toxicology* 8 (1-2): 11985; -42.
- Park JS, Han TS; Lee KY, Han SS, Hwang JJ, Moon DH, Kim SY and Cho YW. N-acetyl histidine-conjugated glycol chitosan self-assembled nanoparticles for intracytoplasmic delivery of drugs: endocytosis, exocytosis and drug release. *J Control Release* 115: 2006; 37-45.

\*\*\*\*\*

